InAs-based quantum cascade lasers grown on on-axis (001) silicon substrate

Z. Loghmari, J.-B. Rodriguez, A. Baranov, M. Rio-Calvo, L. Cerutti, A. Meguekam, M. Bahriz, R. Teissier, E. Tournié

APL Photonics

InAs-based quantum cascade lasers grown on on-axis (001) silicon substrate

Cite as: APL Photonics **5**, 041302 (2020); https://doi.org/10.1063/5.0002376
Submitted: 24 January 2020 . Accepted: 25 March 2020 . Published Online: 14 April 2020

Z. Loghmari, J.-B. Rodriguez, A. N. Baranov, M. Rio-Calvo, L. Cerutti, A. Meguekam, M. Bahriz, R. Teissier, and E. Tournié

InAs-based quantum cascade lasers grown on on-axis (001) silicon substrate

Cite as: APL Photon. 5, 041302 (2020); doi: 10.1063/5.0002376
Submitted: 24 January 2020 • Accepted: 25 March 2020 •
Published Online: 14 April 2020

Z. Loghmari, J.-B. Rodriguez, A. N. Baranov,[a] M. Rio-Calvo, L. Cerutti, A. Meguekam, M. Bahriz, R. Teissier, and E. Tournié

AFFILIATIONS

IES, University of Montpellier, CNRS, F-34000 Montpellier, France

[a]Author to whom correspondence should be addressed: baranov@univ-montp2.fr

ABSTRACT

We present InAs/AlSb quantum cascade lasers (QCLs) monolithically integrated on an on-axis (001) Si substrate. The lasers emit near 8 μm with threshold current densities of 0.92–0.95 kA/cm^2 at 300 K for 3.6-mm-long devices and operate in pulsed mode up to 410 K. QCLs of the same design grown for comparison on a native InAs substrate demonstrated a threshold current density of 0.75 kA/cm^2 and the same maximum operating temperature. The low threshold current density of the QCLs grown on Si makes them suitable for photonic integrated sensor implementation.

Integrating mid-infrared (IR) semiconductor lasers onto silicon platforms is highly desired for the development of compact, cost-effective, smart sensor systems.[1] The direct epitaxial growth of III–V emitters on silicon substrates is better suited for mass-scale production than their heterogeneous integration,[2] but this monolithic approach is complicated by the difference in the crystal structure and a large lattice mismatch between Si and the III–V materials usually employed in semiconductor lasers. Indeed, there are only a few reports on electrically pumped mid-IR lasers directly grown on Si. GaSb-based quantum well lasers operating at 2 μm in the continuous wave (cw) regime above room temperature (RT) have been first demonstrated.[3] More recently, we have also reported the first quantum cascade lasers (QCLs) directly grown on Si.[4] These InAs-based devices emitting near 11 μm exhibited RT threshold current densities Jth of 1.3 kA/cm^2 and operated in pulsed mode up to 380 K, which was close to the characteristics of QCLs grown on a native InAs substrate.[4] InP-based QCLs grown on a silicon substrate have also been subsequently reported, but their performance was much poorer than that of similar devices fabricated on InP substrates.[5] These lasers emitting at 4.35 μm operated in pulsed mode only up to 170 K with a Jth of 1.85 kA/cm^2 at 80 K.

In order to suppress the formation of antiphase domains (APDs) caused by the different crystal structures of non-polar Si substrates and polar III–V compound epitaxial layers,[6] these mid-IR lasers were all grown on silicon substrates exhibiting a large miscut angle (>6°) with respect to the (001) orientation. This makes them incompatible with the standard industrial process based on on-axis (001) Si wafers. In this letter, we report the first QCLs directly grown on an on-axis silicon substrate.

The active zone of the InAs/AlSb QCLs is based on vertical transitions in four coupled quantum wells and resonant phonon extraction. It was designed to emit around 7.5 μm, a region rich in strong absorption features of different molecules.[7] It contains 40 repetitions of the following layer sequence in Å, starting from the injection barrier: **21**/69/**3**/56/**3.5**/54/**4.5**/51/**7**/48/**8**/46/**9**/46/**12**/42/**13**/39/**18**/37, where AlSb layers are in bold and the Si-doped layers (n = 6 × 10^{16} cm^{-3}) are underlined. The total electron sheet density in the structure, taking into account residual doping of InAs (n ~ 8 × 10^{15} cm^{-3}, estimated), is considered to be 1 × 10^{11} cm^{-2} per period. The plasmon enhanced dielectric waveguide of the laser was formed by 2-μm-thick cladding layers made of n-InAs doped with Si to n = 4 × 10^{18} cm^{-3}, separated from the active zone by undoped InAs spacers of the same thickness in order to reduce the overlap of the guided mode with the absorbing doped material. The electromagnetic modeling of the guided modes, using a finite element solver, gives an overlap of the fundamental mode

with the active region Γ = 55% and the waveguide loss α = 3 cm^{-1} for an empty waveguide.

The QCL structure (EQ609) was grown in a RIBER 412 solid-source molecular-beam epitaxy (MBE) reactor equipped with As and Sb valved cracker cells. InAs and AlSb layers were grown using deposition rates of 3.03 Å/s and 1 Å/s, respectively, and a V/III flux ratio of 2 on a GaSb-on-Si template prepared in a separate growth run as follows. Prior to growth, the (001) Si substrate exhibiting a ~0.5° residual miscut was annealed at 1000 °C for 10 min under ultra-high vacuum in a dedicated preparation chamber before being vacuum transferred into the III–V epitaxy chamber where a 1.5 μm GaSb buffer layer was grown underneath the QCL structure. This GaSb-on-Si template was inspected before being reloaded into the MBE reactor for growth of the QCL structure. After thermal oxide removal from the GaSb surface under Sb_2 flux at 560 °C, the growth of the full QCL structure was performed at a temperature of ~450 °C. In addition, a similar QCL structure (EQ746) was grown under the same conditions in a separate growth run on an InAs substrate for the sake of comparison.

The surface morphology of the QCL structure grown on Si was evaluated by atomic force microscopy (AFM) and scanning electron microscopy (SEM). The corresponding images are shown in Figs. 1 and 2(a), respectively. The surface morphology of the wafer was much better than that of the previous QCLs grown on a Si substrate with a 6° miscut [Fig. 2(b), sample from Ref. 4], but the surface was nevertheless quite rough. The rms roughness measured by AFM is 9.9 nm. On the other hand, no antiphase domains were visible in the AFM images, which is ascribed to the high-temperature preparation of the Si substrate. The grown wafers were processed into ridge lasers using wet etching and standard photolithography, the ridge width w being varied between 9 μm and 17 μm. Hard baked photoresist was employed for electrical insulation. The laser ridges were etched down to the bottom n^+-InAs cladding layer. Electrical contacts were formed on the top of the ridges and on the etched part of the wafer using non-alloyed Ti/Au metallization. The Si substrate was thinned down to 50 μm by mechanical polishing, and the wafer was cleaved to form 3.6-mm-long Fabry–Perot lasers. The lasers were then soldered with indium on copper heatsinks, wire-bonded, and tested in pulsed mode (333 ns, 12 kHz). Emission spectra of the devices were measured using a Bruker V70 infrared Fourier transform spectrometer (FTIR). No special selection was made to choose the lasers for measurements. Electrical contacts to the devices fabricated from the QCL wafer grown on InAs were taken on the top of the ridges and at the back of the substrate.

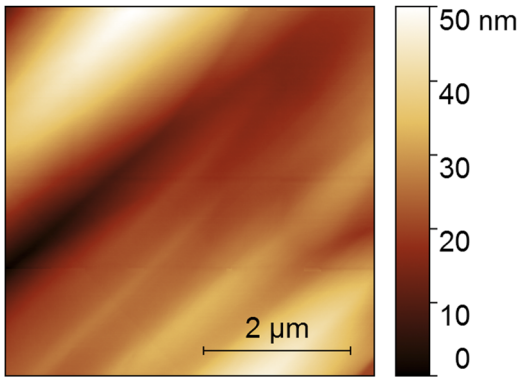

FIG. 1. AFM image of the EQ609 surface (rms roughness 9.9 nm).

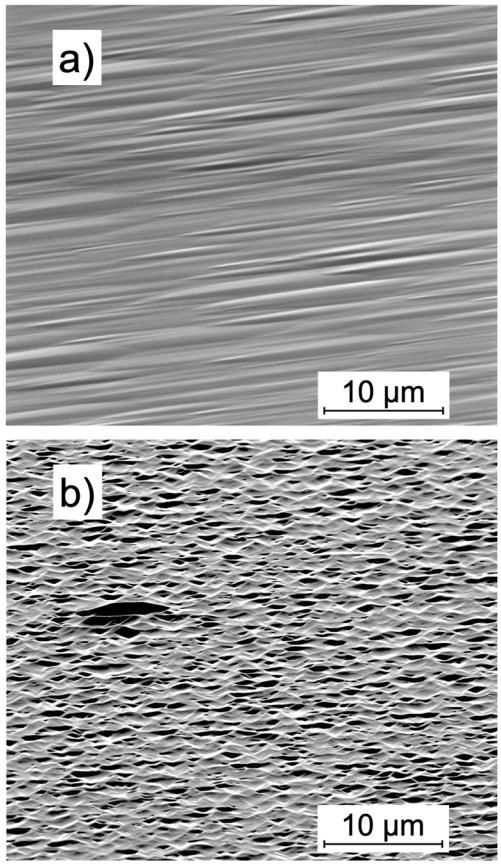

FIG. 2. SEM images of the QCL structures grown on Si. (a) This work (on-axis Si substrate). (b) Sample from Ref. 4 (6°off Si substrate).

The QCLs grown on Si had RT pulsed threshold current densities in the 0.92–0.95 kA/cm^2 range and operated up to a temperature of 410 K (Fig. 3). The reference devices grown on InAs exhibited threshold current densities around 0.75 kA/cm^2 at 300 K and also operated up to 410 K (Fig. 4). The temperature dependence of the threshold current density of the tested QCLs is shown in Fig. 4. Straight lines in this figure indicate a slope corresponding to a characteristic temperature of the exponential dependence T_0 = 125 K, identical around RT for lasers grown on both InAs and Si substrates. However, above 340 K, Jth of the QCLs grown on Si increased slowly with temperature. Although dedicated aging studies will be needed to assess device robustness, we noticed that the threshold current density of the lasers measured at 300 K did not change after the high temperature characterizations around 400 K. Typical emission spectra are shown in the inset in Fig. 4. The lasers emitted wavelengths of 7.7 μm and 8.0 μm at 300 K for the lasers grown on InAs and Si, respectively.

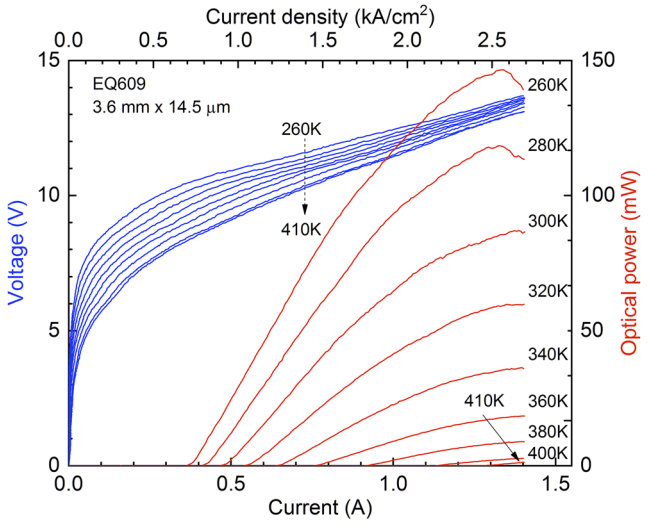

FIG. 3. Voltage–current and light–current characteristics of a QCL grown on a Si substrate measured in pulsed mode at different temperatures.

In general, the operation of InAs/AlSb QCLs grown on silicon can be affected by antiphase boundaries (APBs), delimiting APDs, and threading dislocations originating from the large (≈11%) difference in the lattice parameters of InAs (and AlSb) and Si. A degradation of the performance is therefore expected in these devices compared with QCLs grown on native InAs substrates. The procedure used for preparing the GaSb-on-Si template allowed us to ensure full annihilation of APBs within the 1.5-μm thick GaSb buffer layer sitting well below the QCL active zone, the absence of emerging APBs being confirmed by AFM during preliminary studies. However, the unavoidable high density of threading dislocations (estimated to be in the 10^8 cm^{-2} range from preliminary transmission electron microscopy investigations) does penalize the device performance. Yet, the studied QCLs grown on silicon exhibited RT threshold current densities below 1 kA/cm^2 and only 22% higher than the reference lasers. Both Jth values and their deviation from the values observed on identical devices grown on InAs are smaller than those in the previous InAs/AlSb QCLs that were grown on an off-axis Si substrate, where a 30% increase in Jth was observed.[4] In lasers with short resonators, this difference was even smaller, which was explained by a higher optical gain due to smoother interfaces in the structure grown on an off-axis substrate that favored a step-flow regime of MBE growth. This argument is probably still valid for the lasers studied in this work since the on-axis Si substrate exhibited a residual 0.5° misorientation that can stimulate the step-flow growth mode, thus reducing interface scattering in the QCL structure. A smaller difference in Jth at high temperatures can be considered as an indication of a higher gain in the new lasers grown on Si compared with the devices grown on InAs. However, the most likely explanation of the high QCL performance achieved in this work is the much better crystalline quality of the wafer grown on the on-axis Si substrate (Fig. 2).

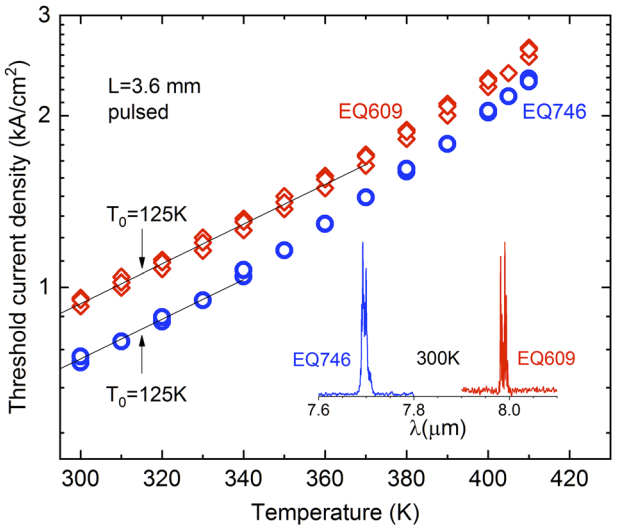

FIG. 4. Threshold current density of QCLs grown on Si (EQ609, w = 13 μm, 14 μm, and 14.5 μm) and on InAs (EQ746, w = 13 μm, and 17 μm) as a function of temperature (semi-logarithmic scale). Emission spectra measured at a current of 0.6 A at 300 K are shown in the inset.

The Jth degradation in QCLs grown on Si can be due to the broadening of the gain curve caused by non-homogeneity of the layer thickness in the active zone of the device. As suggested in Ref. 4, in InAs/AlSb QCLs, this effect is quite weak because of the opposite influence of the fluctuations of the AlSb barriers and InAs wells on the transition energy in the case of their in-phase variations.[4] In order to verify this assumption, we measured spontaneous emission spectra of the devices studied in this work. The spectra were measured at 300 K at a low current density of 0.4 kA/cm^2, corresponding to about 50% of Jth for these devices, in order to avoid narrowing due to the optical amplification (Fig. 5). The full width at half maximum of the spectra extracted from the Lorentzian fits of the data was comparable for both devices, 12.5 meV and 13.5 meV for the lasers grown on InAs and Si, respectively. Measurements on the samples without resonators are necessary for more reliable analysis of the emission linewidth, but the observed trend confirms the conclusion made in Ref. 4. Another reason of the observed increase in Jth of the QCLs grown on silicon can be higher optical losses due to additional absorption on crystal imperfections. This mechanism can similarly explain a weaker performance degradation in short devices observed in Ref. 4.

The reference lasers EQ746 mounted epi-side down operated in the cw regime at temperatures up to 30 °C. At high temperatures, the QCLs EQ609 grown on Si exhibit Jth close to the characteristics of the devices grown on InAs, and they should thus be able to operate under continuous wave operation near RT provided a suitable heat dissipation scheme, such as thick gold plating, is implemented.

In summary, we demonstrated InAs/AlSb quantum cascade lasers monolithically integrated on an on-axis (001) Si substrate. At room temperature, the lasers emitted near 8 μm and exhibited threshold current densities below 1 kA/cm^2, only 22% higher than reference QCLs of the same design grown on a native InAs substrate. The operating temperature of the QCLs grown on silicon reached

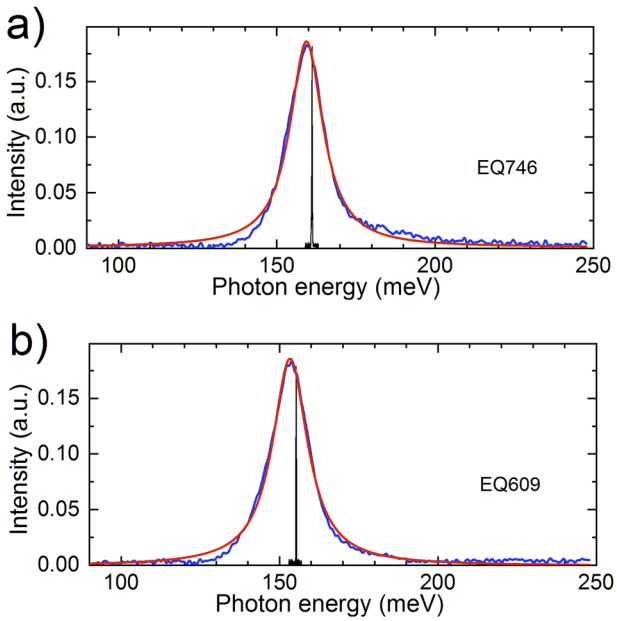

FIG. 5. Emission spectra of the lasers measured at 300 K at a current density of 0.4 kA/cm^2 (~0.5 Jth) and above the threshold (black lines). Red curves show Lorentzian fits of the spectra.

410 K, demonstrating the same performance as the reference devices. The low threshold current density of these devices makes them suitable for photonic integrated sensor implementation. Even though at this stage, the substrate preparation process is not fully CMOS compatible, various remotely controlled sensor chips can already be envisioned based on the co-integration of QCLs and quantum cascade detectors on the same Si photonic circuit or III–V-on-Si photonic circuit.

Part of this work was funded by the H2020 Program of the European Union (REDFINCH, Grant No. 780240) and the French Program "Investment for the Future" (Equipex EXTRA, Grant No. ANR-11-EQPX-0016).

REFERENCES

[1]R. Soref, Nat. Photonics **4**, 495 (2010).
[2]A. Spott, J. Peters, M. L. Davenport, E. J. Stanton, C. D. Merritt, W. W. Bewley, I. Vurgaftman, C. S. Kim, J. R. Meyer, J. Kirch, L. J. Mawst, D. Botez, and J. E. Bowers, Optica **3**, 545 (2016).
[3]J. R. Reboul, L. Cerutti, J. B. Rodriguez, P. Grech, and E. Tournié, Appl. Phys. Lett. **99**, 121113 (2011).
[4]H. Nguyen-Van, A. N. Baranov, Z. Loghmari, L. Cerutti, J.-B. Rodriguez, J. Tournet, G. Narcy, G. Boissier, G. Patriarche, M. Bahriz, E. Tournié, and R. Teissier, Sci. Rep. **8**, 7206 (2018).
[5]R. Go, H. Krysiak, M. Fetters, P. Figueiredo, M. Suttinger, X. M. Fang, A. Eisenbach, J. M. Fastenau, D. Lubyshev, A. W. K. Liu, N. G. Huy, A. O. Morgan, S. A. Edwards, M. J. Furlong, and A. Lyakh, Opt. Express **26**, 22389 (2018).
[6]H. Kroemer, J. Cryst. Growth **81**, 193 (1987).
[7]I. E. Gordon, L. S. Rothman, C. Hill, R. V. Kochanov, Y. Tan, P. F. Bernath, M. Birk, V. Boudon, A. Campargue, K. V. Chance, B. J. Drouin, J.-M. Flaud, R. R. Gamache, J. T. Hodges, D. Jacquemart, V. I. Perevalov, A. Perrin, K. P. Shine, M.-A. H. Smith, J. Tennyson, G. C. Toon, H. Tran, V. G. Tyuterev, A. Barbe, A. G. Császár, V. M. Devi, T. Furtenbacher, J. J. Harrison, J.-M. Hartmann, A. Jolly, T. J. Johnson, T. Karman, I. Kleiner, A. A. Kyuberis, J. Loos, O. M. Lyulin, S. T. Massie, S. N. Mikhailenko, N. Moazzen-Ahmadi, H. S. P. Müller, O. V. Naumenko, A. V. Nikitin, O. L. Polyansky, M. Rey, M. Rotger, S. W. Sharpe, K. Sung, E. Starikova, S. A. Tashkun, J. V. Auwera, G. Wagner, J. Wilzewski, P. Wcisło, S. Yu, and E. J. Zak, J. Quant. Spectrosc. Radiat. Transfer **203**, 3 (2017).